2016

# Investigation of Evaporator Performance with and without Liquid Overfeeding

Stefano Bortolin
*University of Padova, Italy*, stefano.bortolin@unipd.it

Marco Rossato
*University of Padova, Italy*, marco.rossato.1@studenti.unipd.it

Stefano Bernardinello
*Blue Box – Swegon, Italy*, Stefano.Bernardinello@Swegon.it

Davide Del Col
*University of Padova, Italy*, davide.delcol@unipd.it

# Investigation of Evaporator Performance Improvement by Liquid Overfeeding

Stefano BORTOLIN[1*], Marco ROSSATO[1], Stefano BERNARDINELLO[2], Davide DEL COL[1]

[1]University of Padova, Department of Industrial Engineering,
Via Venezia, 1 – 35131 Padova, Italy

[2]Blue Box Group S.r.l. – Swegon Group,
Via Valletta, 5 - 30010 Cantarana di Cona (VE), Italy

*Corresponding Author
Tel.: +39 049 8276885; Fax: +39 049 8276896; E-mail: stefano.bortolin@unipd.it

## ABSTRACT

In the present work, the performance of a segmentally baffled shell-and-tube evaporator working with liquid overfeeding is investigated. The refrigerant is R134a that flows inside the tubes, while water flows on the shell side. A single shell pass has been adopted for the water with one tube pass for the evaporating fluid. The test rig used for the experimental measurements consists of a primary refrigerant loop plus the condenser and the evaporator water auxiliary loops. The evaporator can be fed with two-phase mixture from the expansion valve or with saturated liquid coming from the liquid-vapor separator (in this case a variable speed recirculation pump is used). Inlet and outlet temperatures have been measured for both fluids together with the flow rate allowing the determination of the overall heat transfer coefficient. In addition, pressure drop have been measured on the refrigerant side. Tests have been performed both without overfeeding and with overfeeding at different values of recirculation ratio. The recirculation ratio is defined as the ratio between refrigerant flow rate at the evaporator and the vaporized refrigerant flow rate. Furthermore, measurements have been taken at fixed water outlet temperature and varying the heat duty. In order to study the evaporator behavior, a computational procedure has been developed. Finally, the numerical model of the heat exchanger has been validated against experimental data.

## 1. INTRODUCTION

Liquid overfeed or liquid recirculation refers to the practice of delivering a greater rate of liquid refrigerant to the evaporator than the rate that actually evaporates. Liquid overfeed is common in large-scale industrial refrigeration systems. The major benefit of liquid recirculation is the improvement of the heat transfer coefficient in the evaporator. In fact, in the case of dry expansion systems, a part of the heat exchanger area can be affected by dryout conditions and a further tube length is dedicated to the superheating of the vapor. Both the regions are characterized by low values of the heat transfer coefficients compared with the heat transfer coefficients that can be achieved during flow boiling. The improvement of evaporator heat transfer capabilities by liquid overfeeding is due to the absence of dryout phenomena, no need of superheating and higher refrigerant velocity inside the tubes. Furthermore, feeding the evaporator with liquid only can also improve the refrigerant distribution. However, there are also some disadvantages in such practice: the greater refrigerant charge in the heat exchanger and in the liquid-vapor separator, and the additional pumping power required by the system.
The schematic of a forced liquid recirculation cycle is presented in Figure 1. An externally driven mechanical pump is used to provide the necessary liquid recirculation effect. The pump draws liquid from a liquid-vapor separator and supplies it to the inlet of the evaporator. This type of cycle offers a significant advantage: more liquid is sent to the evaporator than is actually evaporated, meaning that at the outlet of the evaporator there is a two-phase fluid rather than a superheated vapor, as is the case in dry expansion (DX) system operation. Saturated vapor enters the compressor coming from the vapor-liquid separator.

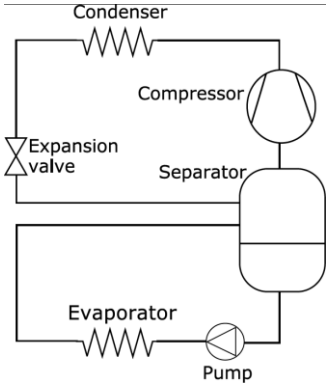


**Figure 1:** Forced liquid recirculation cycle in which a mechanically driven pump is used to provide excess liquid to the evaporator.

Recently, Lawrence and Elbel (2014) presented the results of an experimental and numerical study on the effect of liquid recirculation on the performance of air conditioning cycles. The purpose of the numerical model was to simulate the behavior of a refrigeration cycle (for air conditioning) with forced recirculation of liquid, using R410A as refrigerant. Their model considers a single-pass microchannel evaporator, with 23 parallel tubes, without accounting for maldistribution problems. The evaporator exchanges heat with air. On the air-side, fins are used to increase the heat transfer coefficient. The authors reported that the COP (coefficient of performance) of the cycle increases when increasing the recirculation ratio *R*, with a maximum improvement of about 10%. Furthermore, for *R* > 2.3 the COP shows a smaller variation. The parameter *KA* for the evaporator (that is the product of evaporator global heat transfer coefficient by the heat exchanger area) was found to increase when *R* increases. They suggested that COP improvement of the recirculation cycle with respect to the dry expansion (DX) case is due to the *KA* enhancement. Lawrence and Elbel (2014) performed experimental tests in a R410A air conditioning system with forced liquid recirculation. The evaporator is a microchannel evaporator with similar characteristics of the evaporator considered in their numerical model. The condenser is a round-tube-plate-fin heat exchanger. The cooling capacity, in the various experimental tests, was approximately 0.9 kW, the air temperature at condenser inlet was 35°C and the air temperature at evaporator inlet was 27°C. The author asserted that it was difficult to obtain stable pump operation at very low pump speed, so results were reported only for higher recirculation ratios. Their experimental results shows that the measured *KA* is pretty constant with *R*, as it is expected by the numerical model for high *R* values. For *R* greater than 6, the product *KA* decreases.
The present paper aims at the experimental investigation of the performance of a segmentally baffled shell-and-tube evaporator when working both in dry expansion mode and with liquid overfeeding. The refrigerant R134a flows inside the tubes, beside water flows on the shell side providing the evaporation heat. In the first part of the work, the results of the experimental campaign are reported and discussed. In order to investigate the advantages due to the liquid recirculation, the performance of the evaporator in forced recirculation is compared to the performance in dry expansion mode considering two different heat duties. Finally, in the second part, a numerical model of the heat exchanger has been developed and its results have been validated against experimental data.

## 2. EXPERIMENTAL TEST RIG

The experimental results reported in this paper have been obtained at the facility located at the Research and Development (R&D) laboratory of Blue Box in Cantarana (VE). The test rig allows to perform heat transfer and pressure drop measurement on heat exchangers changing the refrigerant inlet conditions and varying the secondary fluid (water) flow rate and inlet temperature. A schematic of the test rig is reported in Figure 2. In particular, the connections between the different components allow to test the evaporator in direct expansion mode (DX) or in recirculation mode (RC).
In DX mode (represented with a dotted line) the refrigerant:

- flows through the screw compressor;
- is cooled down by water in a condenser;
- flows through the expansion valve;
- absorbs heat from water in the evaporator before reaching again the compressor.

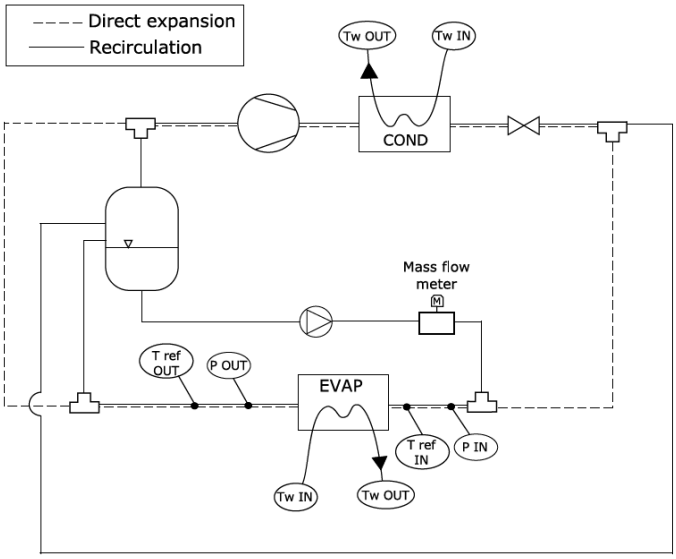


**Figure 2:** Sketch of the test rig used for the measurements of the evaporator performance available at the Blue Box laboratory. Dotted lines for DX mode and continuous lines in the case of RC operation mode.
[T ref (refrigerant temperature); Tw (water temperature); P (pressure)].

**Table 1:** Shell-and-tube evaporator specifications.

| Tubes type | Microfin |
|---|---|
| Tube Outside diameter [mm] | 8.52 |
| Tube inside diameter at fin tip [mm] | 7.44 |
| Fins number | 55 |
| Fin height [mm] | 0.25 |
| Apex angle [°] | 40 |
| Helix angle [°] | 18 |
| Tube layout pattern | 30° triangular |
| Tube length [m] | 3.30 |
| Shell internal diameter [mm] | 263 |
| Tube pitch [mm] | 10 |
| Number of baffles | 21 |
| Baffle type | Segmental |
| Baffle spacing [mm] | 150 |
| Baffle cut [%] | 28 |
| Tube side internal volume [L] | 39.5 |
| External side volume [L] | 137.6 |

The thermostatic expansion valve controls the working condition by maintaining the desired superheat at the outlet of the evaporator.
In RC mode (represented with a continuous line), the refrigerant coming from the condenser enters a vapor-liquid separator tank. Here vapor and liquid phases are separated:

- the liquid goes through a pump that pushes it into the evaporator, after which it flows back to the separator;
- the vapor phase in the upper part of the tank flows through the suction line of the compressor.

A Coriolis effect mass flow meter (expanded uncertainty ±0.004 kg $s^{-1}$) is used to measure the liquid mass flow rate in RC mode. An electromagnetic flow meter is employed for the measurement of the water volumetric flow rate (expanded uncertainty ±0.5% of flow rate). Resistance temperature detectors (RTDs, expanded uncertainty ±0.05°C) and pressure transducers (expanded uncertainty ±4 kPa) have been installed in the refrigerant lines before the inlet

and after the outlet of the evaporator. The water temperature is measured at the inlet and outlet of the heat exchanger (expanded uncertainty ±0.05°C). For all the expanded uncertainties, a coverage factor equal to 2 has been considered.
The heat exchanger here investigated is a segmentally baffled shell-and-tube evaporator using 7.44 mm (inside diameter at the fin tip) copper microfin tubes. The refrigerant R134a flows inside the tubes and the water flows on the shell side. The water can flow in cocurrent or in countercurrent flow depending on the test conditions. A single shell pass with one tube pass is adopted. The general features and dimensions of the heat exchanger are given in Table 1.

## 3. EXPERIMENTAL RESULTS

In this section, the experimental results carried out at Blue Box laboratory are presented. Tests have been run at two different heat duties at the evaporator: 180 kW and 90 kW. A current trend of refrigeration industry is to optimize the energy performances by avoiding intermittent on/off operation mode and moving towards an efficient and continuous operation in a wide range of conditions. Hence, the operation of the evaporator at reduced load is of great interest. The water volumetric flow rate is maintained constant during all the performed tests and the outlet water temperature is fixed at 7°C. This conditions are obtained controlling the water temperature at the inlet of the evaporator.
The evaporator can work in two different modes: dry expansion (DX) and with liquid recirculation (RC). In the first case, the refrigerant enters the evaporator at a constant vapor quality $x$ = 0.2 that is obtained controlling the outlet pressure and the subcooling degree at the condenser. For the direct expansion case, a countercurrent flow evaporator is always considered.
When operating with liquid recirculation, the evaporator is fed with subcooled liquid ($\Delta t_{sub}$~1-2°C) and the refrigerant flow rate can be varied changing the pump velocity (Figure 2). R134a exits from the evaporator in two-phase state with vapor quality depending on the recirculation ratio $R$. The recirculation ratio $R$ is defined as the ratio of the total evaporator mass flow rate to the mass flow rate of vaporized refrigerant and it is an index of the liquid quantity that overfeeds the evaporator.

$$R = \frac{\dot{m}_{evap,total}}{\dot{m}_{evap,vaporized}} \tag{1}$$

It must be noted that tests with liquid recirculation have been taken both in countercurrent flow and in cocurrent flow.

### 3.1 Data reduction

Evaporation is achieved by transferring heat from the secondary fluid (water) that flows in the shell side. The heat flow rate at the evaporator $q_{evap}$ is obtained according to equation 2:

$$q_{evap} = \rho_{water} \dot{V}_{water} c_{water} \left( t_{water,IN} - t_{water,OUT} \right) \tag{2}$$

where the water density $\rho$ and the specific heat $c$ are calculated at the water mean temperature.
When operating in dry expansion mode, since heat losses along the pipes are negligible, the refrigerant enthalpy at the evaporator inlet is considered equal to the enthalpy at the expansion valve inlet, which is calculated with NIST Refprop 9.1 (Lemmon *et al*., 2013) from temperature and pressure measurements of the subcooled liquid at condenser exit. The R134a mass flux in the evaporator when working in dry expansion mode is equal to the refrigerant mass flow rate at the condenser. Therefore, the evaporator mass flux can be obtained from a heat balance performed at the condenser once the following quantities are measured: water volumetric flow rate, water inlet and outlet temperature difference, refrigerant inlet and outlet temperature and pressure (superheated vapor and subcooled liquid state).
Instead, during liquid tests with liquid overfeeding, the refrigerant enthalpy at the inlet of the evaporator is obtained from the pressure and temperature measurements of the subcooled liquid and the refrigerant mass flow rate is directly measured after the recirculation pump as illustrated in Figure 2. Once the refrigerant flow rate is known, the outlet R134a enthalpy is calculated with the following equation:

$$h_{evap,OUT} = h_{evap,IN} + \frac{q_{evap}}{\dot{m}_{R134a}} \tag{3}$$

Finally, the thermodynamic vapor quality at the inlet and outlet of the evaporator $x$ is calculated by equations 4, where $h_{liq}$ and $h_{vap}$ are respectively the specific enthalpy of saturated liquid and saturated vapor computed at inlet and outlet pressure.

$$x_{IN} = \frac{h_{IN} - h_{liq}}{h_{vap} - h_{liq}} \qquad x_{OUT} = \frac{h_{OUT} - h_{liq}}{h_{vap} - h_{liq}} \tag{4}$$

It should be noted that both pressure and temperature are measured at the inlet and the outlet of the evaporator as reported in Figure 2.

### 3.2 Evaporator performance

In Figure 3 the saturation temperature obtained from the pressure measured at the inlet of the evaporator is reported as a function of the relative recirculation ratio $R^*$. The parameter $R^*$ is equal to zero in DX mode whereas in RC mode it is defined as in equation 5

$$R^* = \frac{R-1}{R_{\max}-1} \cdot 100 \tag{5}$$

where $R_{max}$ is the recirculation ratio that is possible to achieve with the pump running at the maximum speed.
When $R^* = 0$ the evaporator works in dry expansion mode whereas for $0 < R^* < 100\%$ the evaporator is overfed with liquid. For both the heat duties considered (180 kW and 90 kW), the inlet evaporation temperature was found to increase when adopting liquid recirculation. However, there is a recirculation ratio beyond which a further increase of $R$ does not lead to a higher evaporation temperature.
Figure 4 reports the vapor quality at the inlet and outlet of the evaporator as a function of the refrigerant mass velocity $G$. For each heat flow rate, the lowest value of mass velocity corresponds to the case of dry expansion (inlet vapor quality $x = 0.2$). As expected, since the heat flow rate is fixed, the outlet vapor quality decreases when the mass velocity and thus the recirculation ratio are increased.

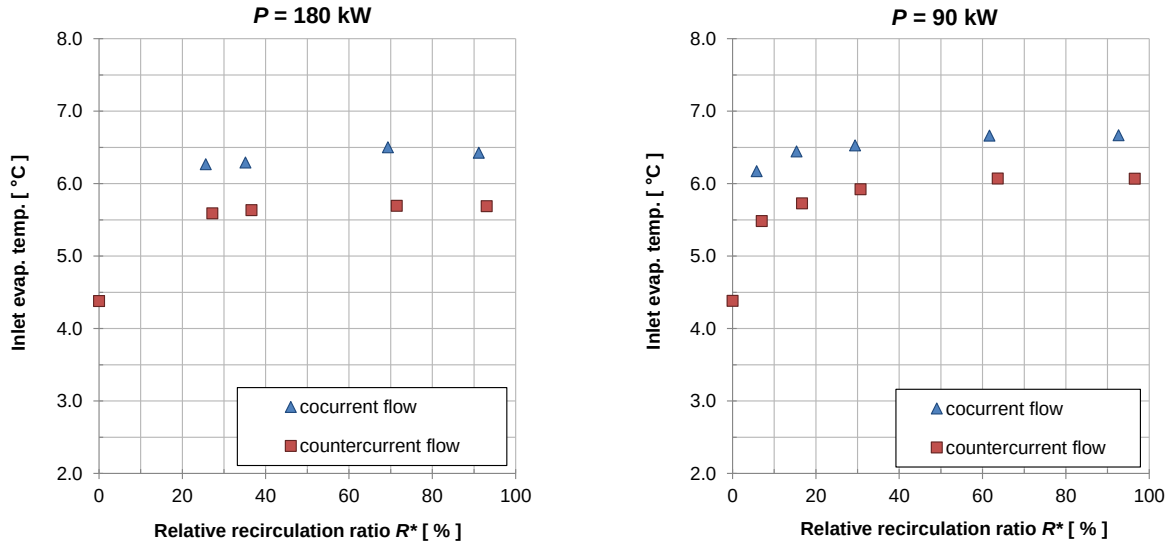


**Figure 3:** Saturation temperature at evaporator inlet versus relative recirculation ratio $R^*$ ($R^* = 0$ in the case of dry expansion). Tests with liquid recirculation ($R^* > 0$) have been performed with water in cocurrent and countercurrent flow. Left: heat duty 180 kW. Right: heat duty 90 kW.

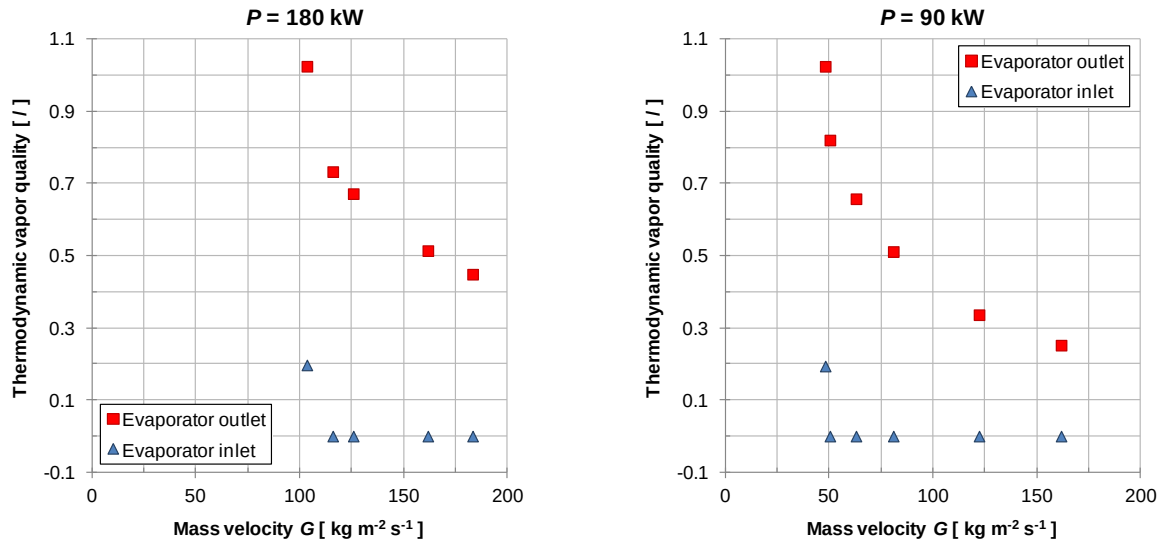


**Figure 4:** Thermodynamic vapor quality at evaporator inlet and exit plotted versus refrigerant mass velocity *G* (the minimum value of *G* corresponds to the case of dry expansion) with water in countercurrent flow. Left: heat duty 180 kW. Right: heat duty 90 kW.

Since during phase change pressure drop affects also the evaporation temperature, in Figure 5 the measured refrigerant pressure drop between inlet and outlet is reported versus the relative recirculation ratio *R**. A pressure drop reduction is found when liquid overfeed is used with respect to the dry expansion case. This can be explained considering that, with liquid recirculation, the dryout zone and the superheating zone in the evaporator are not present and furthermore the exit vapor quality is reduced (Figure 4). Considering *R** > 0, an increase of the recirculation ratio leads to an increase of the pressure drop. Higher pressure drop values have been observed in the case of water in cocurrent flow.

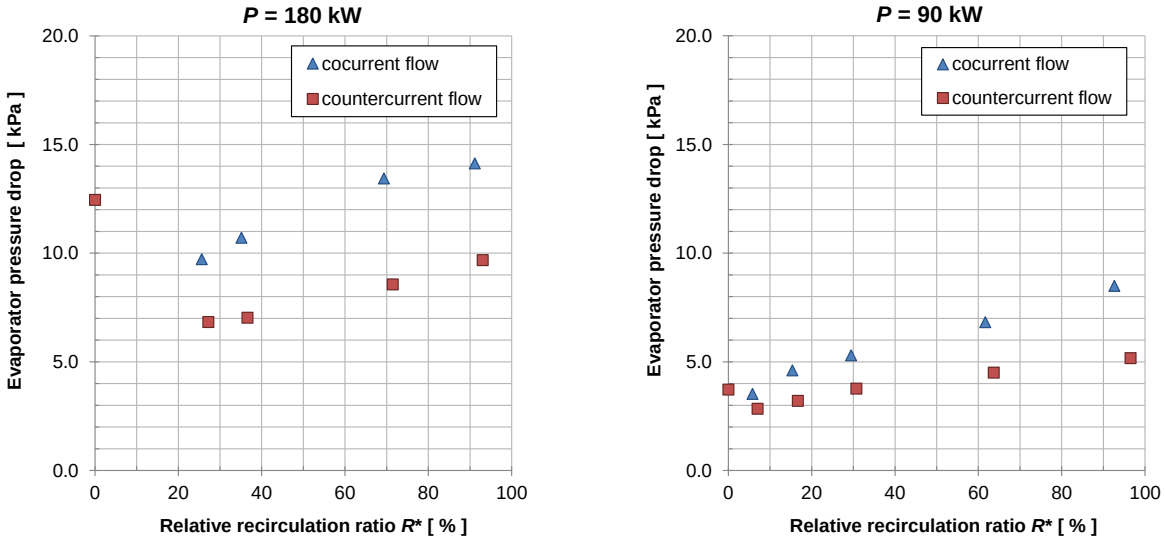


**Figure 5:** Pressure drop in the evaporator versus relative recirculation ratio *R** (*R** = 0 in the case of dry expansion). Tests with liquid recirculation (*R** > 0) have been performed with water in cocurrent and countercurrent flow. Left: heat duty 180 kW. Right: heat duty 90 kW.

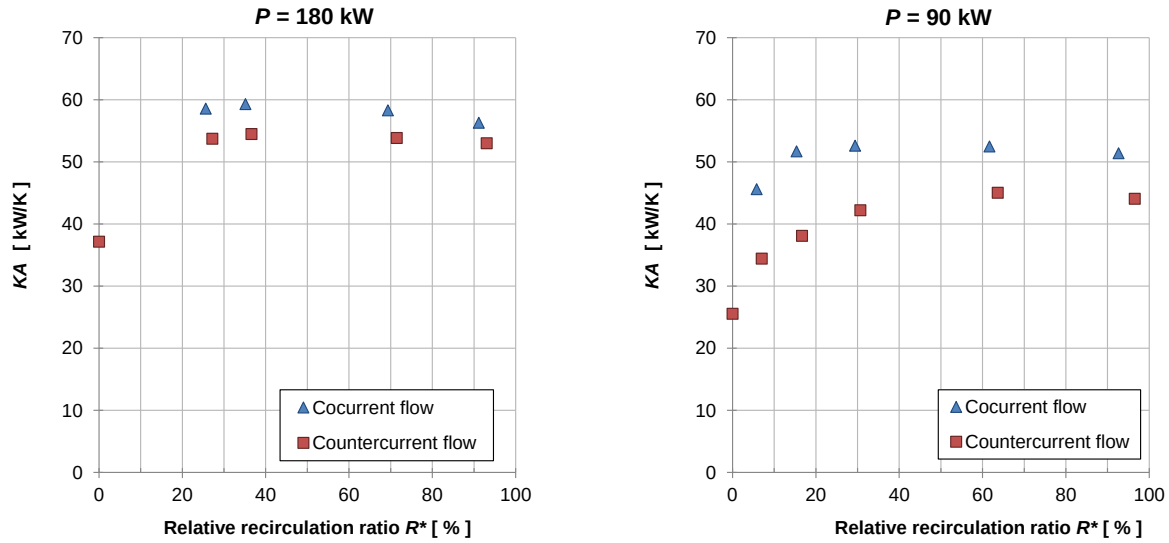


**Figure 6:** Product of the overall heat transfer coefficient by the heat transfer area (*KA*) versus relative recirculation ratio *R** (*R** = 0 in the case of dry expansion). Tests with liquid recirculation (*R** > 0) have been performed with water in cocurrent and countercurrent flow. Left: heat duty 180 kW. Right: heat duty 90 kW.

The heat transfer behavior of the evaporator can be evaluated considering the parameter *KA* that is the product of the overall heat transfer coefficient by the heat transfer area. Considering the graphs in Figure 6, the evaporator shows a performance improvement when working with liquid overfeeding. The *KA* enhancement is more evident at 90 kW. This is due to the fact that, in the direct expansion mode at partial loads, the refrigerant velocity inside the evaporator is reduced leading to low values of the internal heat transfer coefficient. There is an optimum value of the recirculation ratio (that depends on the heat duty) that gives the highest *KA*. Anyhow, when liquid recirculation is adopted and thus no superheating is needed, the best evaporator configuration is the one with water in cocurrent flow.

## 4. MODEL OF THE EVAPORATOR

The modeling of an evaporator is rather complex because of the many heat transfer mechanisms occurring from inlet to outlet. However, a good approximation can be made when considering three regions on the refrigerant side, with different heat transfer features, i.e. the evaporating region, the dryout region and the superheat region. Depending on the conditions (dry expansion or liquid recirculation) the dryout region and the superheat zone can be or not be present in the heat exchanger. Each region was further discretized into several subsectors along the tube length in each of them the heat transfer coefficient and the pressure gradient can be considered constant. In the two-phase region, since the heat transfer coefficient depends on local vapor quality, the length of each subsector varies to maintain a fixed vapor quality change $\Delta x$ in each subsector. The thermodynamic and transport properties of the R134a have been computed from the NIST Refprop 9.1 database (Lemmon *et al*., 2013).

The heat transfer rate (180 kW or 90 kW), the outlet water temperature (7°C), the water flow rate, the inlet vapor quality (0.2) and vapor superheating when operating in dry expansion (5 K) are given as inputs to the algorithm, whilst the program output is the inlet evaporating temperature required to fulfill the imposed conditions.

The R134a evaporation heat transfer coefficients have been obtained from the Cavallini *et al*. (1999a) correlation developed for flow boiling inside microfin tubes and modified as reported in Cavallini *et al*. (2006) to extend its range at mass velocities *G* below 100 kg $m^{-2}$ $s^{-1}$. The refrigerant pressure drop in the evaporating and dryout regions has been computed by the Cavallini *et al*. (1999b) correlation. Their model is based on the Friedel (1979, 1980) pressure drop correlation; the presence of fins on the internal surface of the tube is accounted for with a modification of the smooth tube friction factor that depends on the fin height and on the helix angle. The onset of dryout has been calculated as suggested in a recent paper by Padovan *et al*. (2011). In the dryout region, the heat transfer coefficient has been assumed equal to the single phase convective coefficient when the vapor fraction alone flows in the tubes. The pressure drop in the region of superheated vapor has been computed by the Churchill (1977) correlation.

The acceleration pressure drop has been evaluated using the Rouhani (1969) model for the void fraction. The overall heat transfer coefficient and pressure drop on the shell side have been computed by the Bell-Delaware method as published in the HEDH (Taborek, 1983).
The algorithm of the evaporator model consists of several nested loops that are used to lead to convergence the main quantities (saturation temperature, evaporator length, critical vapor quality, pressure drop, etc.). The algorithm can be summarized in the following main steps:
-the water side heat transfer coefficient is obtained by the Bell-Delaware method;
-a guess value is initially used for the saturation temperature;
-the vapor quality at the onset of dryout is estimated considering the whole heat flow rate;
-the R134a heat transfer coefficient and pressure drop gradient are calculated in the subsectors that belongs to the vaporization region;
-the overall heat transfer coefficient (considering refrigerant, wall and water heat transfer resistance) and the length of each subsector are computed;
-the total length of the evaporation region is obtained as the sum of the lengths calculated for each subsector;
-the conditions (saturation temperature, pressure, vapor quality, water temperature) at the inlet of the dryout zone are known;
-the refrigerant heat transfer coefficient and pressure drop in the dryout region are calculated;
-the overall heat transfer coefficient and the heat transfer length in the dryout region are obtained;
-when operating in dry expansion, the refrigerant heat transfer coefficient and pressure drop in the superheating region are calculated;
-the overall heat transfer coefficient and the heat transfer length in the superheating region are obtained;
-finally, the total length of the evaporator is calculated and compared against the effective length: thus the saturation temperature is corrected until the calculated length matches the effective value.
Comparisons between the experimental inlet evaporating temperatures and calculations for the two considered heat flow rates are shown in Figure 7. As it can be seen, a very good agreement is obtained with recirculation when water flows in countercurrent. In cocurrent flow, an underestimation of the evaporation temperature is found in the case of $P$ = 90 kW and mass velocity below 100 kg m$^{-2}$ s$^{-1}$. This can be related to the estimation of the flow boiling heat transfer coefficient at low mass velocity and low vapor qualities. In fact, when operating in cocurrent flow, the highest water-to-saturation temperature difference is at the entrance of the evaporator and therefore an accurate prediction of the heat transfer coefficient in this region is necessary. Unfortunately, low mass velocities are poorly investigated and predictions model can be less accurate at such conditions.

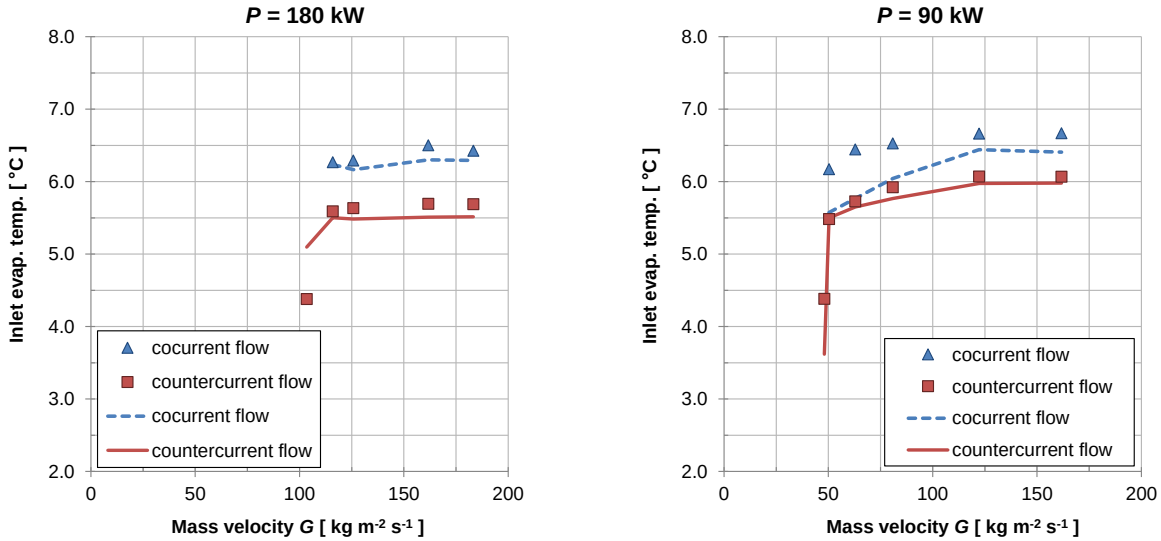


**Figure 7:** Saturation temperature at evaporator inlet versus refrigerant mass velocity $G$ (the minimum value of $G$ corresponds to the case of dry expansion). Tests with liquid recirculation have been performed with water in cocurrent and countercurrent flow. Dots corresponds to measured values, lines show model estimations. Left: heat duty 180 kW. Right: heat duty 90 kW.

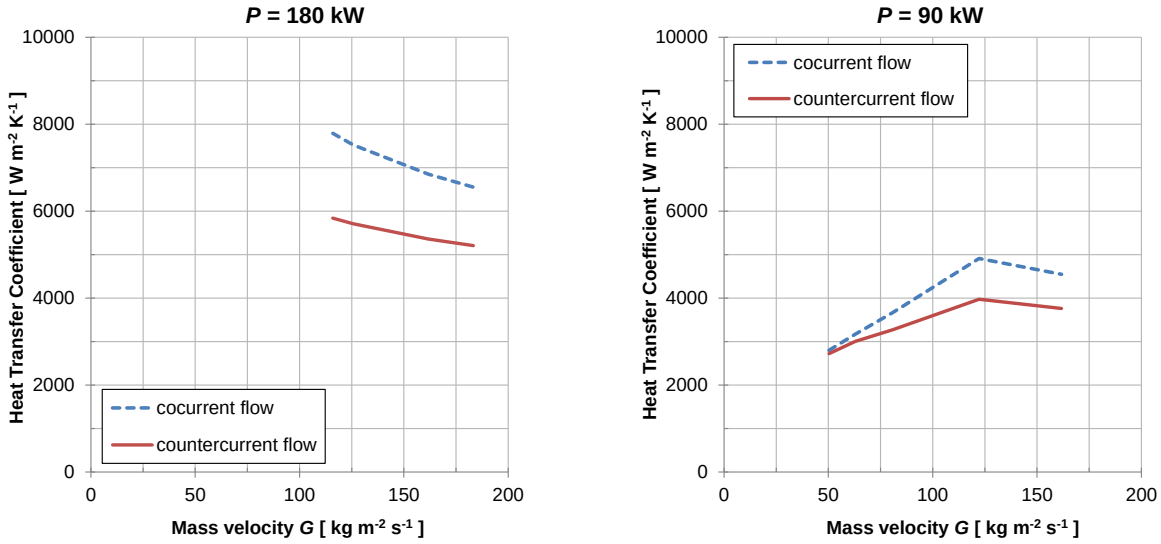


**Figure 8:** Computed mean heat transfer coefficient versus refrigerant mass velocity with liquid overfeeding. Left: heat duty 180 kW. Right: heat duty 90 kW.

In Figure 8, the calculated mean evaporation heat transfer coefficient when considering liquid recirculation is plotted against the refrigerant mass velocity. The recirculation has two opposite effects on the mean heat transfer coefficient. In fact, a higher recirculation ratio and thus a higher mass velocity leads to an increase of the convective boiling heat transfer coefficient. On the other side, increasing the liquid flow rate, as shown in Figure 4, the exit vapor quality is reduced and the heat transfer coefficient decreases. Depending on the opposite action of mass velocity and exit vapor quality, the heat transfer coefficient can decrease with recirculation or it can present a maximum value (as in the case of $P$ = 90 kW).
Finally, another consideration can be done looking at the graphs in Figure 8. The mean heat transfer coefficient is always higher in cocurrent flow with respect to countercurrent flow. It must be noticed that, when the recirculation ratio and the heat duty are fixed, the exit vapor quality is the same in both concurrent and countercurrent flow. Therefore, a higher average heat transfer coefficient in the evaporator means that the evaporator region characterized by low values of the heat transfer coefficient (that is the entrance region with low vapor quality since dryout does not take place with recirculation) is reduced in the case of cocurrent flow. This is caused by the higher water-to-saturation temperature difference encountered at the inlet of the evaporator when it works with water in cocurrent flow.

## 5. CONCLUSIONS

In the present paper, the performance of a shell-and-tube evaporator when working in dry expansion mode or with liquid overfeeding has been experimentally investigated. Furthermore, a numerical model of the evaporator has been proposed and its results have been compared against experimental data. The following conclusions can be drawn:

- At a constant heat duty and fixed exit water conditions, the inlet evaporation temperature increases using liquid recirculation when compared to the case of dry expansion.
- The evaporator heat transfer performance has been evaluated considering the product between the overall heat transfer coefficient and the heat transfer area $KA$. With recirculation, an increase of $KA$ has been found and this is mainly due to the absence of the dryout and superheating zones.
- There is an optimal value of the recirculation ratio that leads to the best evaporation performance; a further liquid flow rate increase leads to a reduction of the $KA$ and to an increase of pressure drop.
- When operating in liquid recirculation, the configuration with water in cocurrent flow leads to higher refrigerant mean heat transfer coefficient.

## NOMENCLATURE

| | | |
|---|---|---|
| $A$ | area | ($m^2$) |
| $c$ | specific heat | (J $kg^{-1}$ $K^{-1}$) |
| $G$ | mass velocity | (kg $m^{-2}$ $s^{-1}$) |
| $h$ | specific enthalpy | (J $kg^{-1}$) |
| $K$ | global heat transfer coefficient | (W $m^{-2}$ $K^{-1}$) |
| $\dot{m}$ | mass flow rate | (kg $s^{-1}$) |
| $P$ | heat duty | (W) |
| $q$ | heat flow rate | (W) |
| $R$ | recirculation ratio | (-) |
| $R^*$ | relative recirculation ratio | (%) |
| $t$ | temperature | (°C) |
| $V$ | volumetric flow rate | ($m^3$ $s^{-1}$) |
| $x$ | vapor quality | (-) |
| ρ | density | (kg $m^{-3}$) |

**Subscript**

| | |
|---|---|
| evap | evaporator |
| IN | inlet |
| liq | saturated liquid |
| max | maximum |
| OUT | outlet |
| sub | subcooled |
| vap | saturated vapor |

## REFERENCES


Cavallini, A., Del Col, D., Doretti, L., Longo, G. A., & Rossetto, L. (1999a). Refrigerant vaporization inside enhanced tubes: a heat transfer model. *Heat and Technology*, 17(2), 29–36.

Cavallini, A., Del Col, D., Doretti, L., Longo, G. A., & Rossetto, L. (1999b). A new computational procedure for heat transfer and pressure drop during refrigerant condensation inside enhanced tubes. *Enhanced Heat Transfer*, 6, 441–456.

Cavallini, A., Del Col, D., & Rossetto, L. (2006). Flow boiling inside microfin tubes: prediction of the heat transfer coefficient. In: *Proceedings of ECI International Conference on Boiling Heat Transfer*, Spoleto, Italy.

Churchill, S.W. (1977). Friction factor equation spans all fluid flow regimes. *Chemical Engineering*, 45, 91–92.

Friedel, L. (1979). Improved friction pressure drop correlations for horizontal and vertical two-phase pipe flow. Proc. Europ. *Two-phase Flow Group Meet*., Ispra, Paper E2.

Friedel, L. (1980). Pressure drop during gas/vapor-liquid flow in pipes. *Int. Chem. Engineering* 20, 352-367.

Lawrence, N. & Elbel, S. (2014). Experimental and numerical study on the performance of R410A liquid recirculation cycles with and without ejectors. In *Proceedings of the 15th International Refrigeration and Air Conditioning Conference at Purdue*, July 14–17 (2187, 10 pages).

Lemmon, E.W., Huber, M.L., & McLinden, M.O. (2013). NIST Standard Reference Database 23: Reference Fluid Thermodynamic and Transport Properties-REFPROP, Version 9.1, National Institute of Standards and Technology, Standard Reference Data Program, Gaithersburg.

Padovan, A., Del Col, D. & Rossetto, L. (2011). Experimental study on flow boiling of R134a and R410A in a horizontal microfin tube at high saturation temperatures. *Applied Thermal Engineering*, 31, 3814–3826.

Rouhani, S.Z. (1969). Subcooled void fraction. AB Atomenergi Sweden, Internal Rept. AE-RTV841.

Taborek, J. (1983). *Heat Exchanger Design Handbook*. Hemisphere P. Corporation.